# FRMD7 Mutations Disrupt the Interaction with GABRA2 and May Result in Infantile Nystagmus Syndrome

Lei Jiang,[1] Yulei Li,[1] Kangjuan Yang,[2] Yuping Wang,[3] Jiuxiang Wang,[1] Xiaoniu Cui,[1] Jinglin Mao,[1] Yong Gao,[1] Ping Yi,[1] Lejin Wang,[4] and Jing Yu Liu[1,5]

[1]Key Laboratory of Molecular Biophysics of the Ministry of Education, College of Life Science and Technology, Huazhong University of Science and Technology, Wuhan, China
[2]Department of Cell Biology and Medical Genetics, Medical School of Yanbian University, Yanji, China
[3]Reproductive Medicine Center, Affiliated Hospital of Yanbian University, Yanji, China
[4]Department of Ophthalmology, Peking University People's Hospital, Beijing, China
[5]Institute of Neuroscience, State Key Laboratory of Neuroscience, Chinese Academy of Sciences Center for Excellence in Brain Science and Intelligence Technology, Chinese Academy of Sciences, Shanghai, China

Correspondence: Jing Yu Liu, Key Laboratory of Molecular Biophysics of the Ministry of Education, College of Life Science and Technology, Huazhong University of Science and Technology, Wuhan, Hubei, 430074, China;
liujy@hust.edu.cn.
Lejin Wang, Department of Ophthalmology, Peking University People's Hospital, Beijing, 100044, China;
13911822021@163.com.

LJ and YL contributed equally to this work.

**Received:** October 11, 2019
**Accepted:** April 13, 2020
**Published:** May 23, 2020

Citation: Jiang L, Li Y, Yang K, et al. FRMD7 mutations disrupt the interaction with GABRA2 and may result in infantile nystagmus syndrome. *Invest Ophthalmol Vis Sci.* 2020;61(5):41.
https://doi.org/10.1167/iovs.61.5.41

**Purpose.** To identify the pathogenic gene of infantile nystagmus syndrome (INS) in three Chinese families and explore the potential pathogenic mechanism of FERM domain-containing 7 (*FRMD7*) mutations.

**Methods.** Genetic testing was performed via Sanger sequencing. Western blotting was used to analyze protein expression of FRMD7. Glutathione S-transferase pull-down and immunoprecipitation were conducted to investigate the proteins interacting with FRMD7. Rescue assays were performed in *Caenorhabditis elegans* to explore the potential role of FRMD7 in vivo.

**Results.** We recruited three Chinese families with X-linked INS and identified a duplication and two missense mutations in *FRMD7*: c.998dupA/p.His333Glnfs*2, c.580G>A/p.Ala194Thr, and c.973A>G/p.Arg325Gly (one in each family). Expression levels of three mutants were similar to that of wild-type FRMD7 in vitro. Interestingly, the mutant p.His333Glnfs*2 exhibited a predominantly nuclear location, whereas wild-type FRMD7 localized to the cytoplasm. In addition, we found FRMD7 to directly interact with the loop between transmembrane domains 3 and 4 of GABRA2, a type A gamma-aminobutyric acid (GABA) receptor ($GABA_A$Rs) subunit critical for receptor transport and localization, whereas the mutants p.Ala194Thr and p.Arg325Gly exhibited decreased binding to GABRA2. In *frm-3* (a nematode homologue of *FRMD7*) null *C. elegans*, we found that FRMD7 mutants exhibited a poor rescue effect on the defects of locomotion and fluorescence recovery after photobleaching of $GABA_A$Rs.

**Conclusions.** Our findings identified three *FRMD7* mutants in three Chinese families with X-linked INS and confirmed GABRA2 as a novel binding partner of FRMD7. These findings suggest that FRMD7 plays an important role by targeting $GABA_A$Rs.

Keywords: X-linked infantile nystagmus, *FRMD7*, GABRA2, *frm-3*, *Caenorhabditis elegans*

Infantile nystagmus syndrome (INS) is an eye movement disorder characterized by involuntary, periodic, and predominantly horizontal oscillations of both eyes. Although visual function can be significantly reduced in INS patients, the degree of impairment varies.[1] To date, three inheritance patterns of INS, including autosomal dominant, autosomal recessive, and X-linked forms, have been reported, with X-linked INS being the most common. FERM domain-containing 7 (*FRMD7*) is identified as the pathogenic gene in approximately 50% of X-linked INS pedigrees and 5% of sporadic patients.[2–7] However, the role of FRMD7 in the pathogenesis of INS remains unclear.

Recently, FRMD7 was found to interact with calcium/calmodulin-dependent serine protein kinase and promote the outgrowth of mouse neuroblastoma 2A (N2A) cell neurites in vitro,[8] and foveal and optic nerve head hypoplasia were observed in *FRMD7* mutant individuals.[9] Those evidences suggest that FRMD7 may participate in neural and retinal development. In addition, loss of horizontal optokinetic reflex (OKR) was observed in *Frmd7* mutant (*Frmd7*$^{tm}$) mice, but no nystagmus was observed, which may be because of the absence of microsaccades in mice.[10] Consistently, loss of OKR associated with *FRMD7* mutations has been characterized in patients.[5,11] OKR and vestibulo-ocular reflexes (VOR) are the two gaze stabilization systems in vertebrates.[12,13] OKR responds to slow-motion stimuli on the retina, whereas VOR responds to head movement stimuli.[14,15] The two systems are coordinated to control

eye movement and stabilize the image on the retina during surrounding-motion or self-motion.[12,16] Disruption of each system might impair coordination and disturb eye movement, such as nystagmus and bilateral vestibular failure.[14,17,18] Furthermore, *Frmd7* is specifically expressed in starburst amacrine cells (SACs), and the directional selective (DS) inhibitory input from SACs to DS ganglion cells (DSGCs) is lost in *Frmd7*$^{tm}$ mice,[10] suggesting an important role for FRMD7 in DS signaling and the generation of OKR.

Inhibitory signals from SACs to DSGCs and from SACs to SACs are dependent on gamma-aminobutyric acid (GABA) transmission and critical for the generation of the DS response in DSGCs.[19] Accordingly, the DS response of DSGCs is absent in *Frmd7*$^{tm}$ mice.[20] Interestingly, a similar phenotype was found in *Gabra2* knockout mice,[21] which led us to investigate whether FRMD7 associates with GABRA2 to contribute to DS signaling. GABRA2 has a common structure similar to other type A GABA receptor ($GABA_A$Rs) subunits, which contain four transmembrane domains (TMs) and a large intracellular loop between TM3 and TM4. The TM3-TM4 loop of the $GABA_A$R $\alpha$ subunit interacts with other proteins to localize $GABA_A$R to postsynaptic membranes or the actin cytoskeleton.[22–26]

Coincidentally, a similar observation was found for the FERM domain-containing protein FRM-3 (nematode homologue of FRMD7) in *Caenorhabditis elegans*, which interacts with UNC-49B (a nematode $GABA_A$Rs subunit) and stabilizes $GABA_A$Rs on the postsynaptic membrane.[27] GABA acts primarily at the neuromuscular synapses of *C. elegans* to relax body muscles during locomotion and foraging.[28]

In this study, we identified three *FRMD7* mutations (c.998dupA/p.His333Glnfs*2, c.580G>A/p.Ala194Thr, and c.973A>G/p.Arg325Gly) in three Chinese families with X-linked INS, among which c.998dupA and c.580G>A are novel. Furthermore, we identified GABRA2 as a novel FRMD7-interacting protein. The FRMD7 mutants exhibited decreased binding affinity or incorrect location in vitro and impaired abilities to rescue the defects of *frm-3* null *C. elegans* in vivo. Our results proposed a novel mechanism of FRMD7 in the pathogenesis of INS.

## Methods

### Study Subjects and Isolation of Genomic DNA

The participants of family 1 were identified and enrolled at the Affiliated Hospital of Yanbian University. Family 2 cases were collected in Nanyang City of Henan Province. Family 3 cases were collected in Jingmen City of Hubei Province. The members of three families participating in this study received ophthalmology examinations by professional ophthalmologists. Informed consent was obtained from all participants in the three families in accordance with the study protocols approved by the ethics committee of Huazhong University of Science and Technology. The research complied with the principles of the Declaration of Helsinki.

Genomic DNA was extracted from peripheral blood samples using Wizard Genomic DNA Purification Kit (Promega, Madison, WI, USA).

### Mutation Analysis

Mutation analysis was performed by polymerase chain reaction (PCR) and Sanger sequencing. Once the mutations were confirmed, cosegregation analysis was performed for the entire family, and mutation screening for healthy control subjects was subsequently carried out.

### Cell Culture and Treatment

Kidney fibroblast cell line (COS7) cells and N2A cells were routinely cultured in antibiotic-free Dulbecco's modified Eagle's medium (Gibco, Gaithersburg, MD, USA) with 10% fetal bovine serum (Gibco). Plasmids were transfected into cells using Lipofectamine 2000 (Invitrogen, Carlsbad, CA, USA).

### Plasmid Construction

The full-length *FRMD7* and *GABRA2* cDNA sequences were amplified from a cDNA template of SH-SY5Y cells. The full-length *FRMD7* and *GABRA2* cDNAs and the sequence of the TM3-TM4 loop of *GABRA2* were cloned into the pEGFP-N1, pcDNA3.1, and pGEX-6P expression vectors, respectively. The mutant *FRMD7* sequences were constructed based on the wild-type *FRMD7* sequence and cloned into pEGFP-N1. The PCR primers used for FRMD7 mutant amplification are as follows:

c.580G>A forward primer: TCAGGCCTCACCCCACCAGTGATGGTGAA
c.580G>A reverse primer: TTCACCATCACTGGTGGGGTGAGGCCTGA
c.973A>G forward primer: CTTGCCATTTGAAGGGAAACATTACCC
c.973A>G reverse primer: GGGTAATGTTTCCCTTCAAATGGCAAG
c.998dupA forward primer: ATCTCAGTACCATAGAACGACAGTGCAG
c.998dupA reverse primer: CTGCACTGTCGTTCTATGGTACTGAGAT

The expression vectors injected into *C. elegans* were based on the pPD49.26 and pPD95.67 backbone. A 3 kb *frm-3* promoter was used to drive green fluorescent protein (GFP)-tagged FRMD7 *or* FRM-3 protein expression in *C. elegans* neurons and body muscles, which was constructed into the pPD95.67 vector. Additionally, 1.5 kb of the *unc-49* promoter was used for expressing UNC-49B-A2loop-fused red fluorescent protein (RFP) in *C. elegans* body muscles, which was constructed into the pPD49.26 vector.

### Western Blot, Glutathione S-Transferase (GST) Pull-Down Assays, and Immunoprecipitation (IP) Assays

COS7 cells were transfected with expression plasmids and lysed with cell lysis buffer (Beyotime Institute of Biotechnology, Nanjing, China) after 24 hours in culture at 37°C.

The GST pull-down assay was performed as previously described.[29] In brief, expression plasmids were transformed into *Escherichia coli* Rosetta cells, and expression of GST-fused protein was induced with isopropyl thiogalactoside at 37°C for 8 hours. The cells were harvested, ultrasound-lysed, and centrifuged at 16000 g to obtain the supernatant. The supernatant containing GST-fused proteins was incubated with glutathione agarose beads at 4°C for 4 hours and then washed three times with phosphate-buffered saline.

The FRMD7 containing lysate was added to the supernatant to be pulled down by the GST-loop.

The IP assay was performed as follows. Protein extracts were obtained from the transfected COS7 cells or C57BL/6 wild-type mouse retinal tissue, and incubated with a primary antibody or IgG at 4°C for 12 hours followed by mixing with protein A agarose beads, and Fast Flow (16-156; Merck Millipore, Billerica, MA, USA) for 4 hours. The immunoprecipitated proteins were obtained by centrifugation at 12,000*g* for 10 minutes and denaturation by boiling for 5 minutes.

Primary antibodies used are as follows: FRMD7 (1:500, rabbit polyclonal antibody; Sigma-Aldrich, St. Louis, MO, USA), GABRA2 (1:500, mouse monoclonal antibody; Abcam, Cambridge, UK), GFP (1:3000, mouse monoclonal antibody; ABclonal, Cambridge, MA, USA), and GST (1:5000, mouse monoclonal antibody; ABclonal).

### Worm Assays

N2 (wild-type) and VC1288 (*frm-3*(*gk585*)) were obtained from the *Caenorhabditis* Genetics Center (CGC, University of Minnesota, Minneapolis, MN, USA) and maintained at 22°C under standard conditions; *E. coli* OP50 was used as food for the worms.[30] Microinjection was carried out as reported previously[31] to obtain transgenic worms. The research confirmed adherence to the ARVO Statement for the Use of Animals in Ophthalmic and Vision Research.

To assess the rate of locomotion, young adult worms were transferred to fresh nematode growth medium (NGM) plates with OP50 and adapted for 5 minutes before filming. The locomotion of worms on NGM plates was screened under a Zeiss Discovery V8 stereomicroscope (Carl Zeiss MicroImaging Gmbh, Göttingen, Germany), and a 1-minute video recording was captured by the Andor iXon$^{EM}$ + DV885K EMCCD camera (Andor, Belfast, UK). The films were converted to an AVI format and analyzed by Multi-Worm Tracker 1.3.0 software (Kerr Lab, Ashburn, Virginia, USA) to calculate the locomotion rate. In the thrashing assay, young adult worms were transferred to a 200 µL centrifuge tube with agar on the bottom and filled with 100 µL M9 buffer. The worms were adapted for 2 minutes before counting thrashing frequency. Thrashing was defined and counted as reported previously.[32]

### FRAP Assay

The FRAP assay was performed as described previously.[27] Briefly, worms were placed on 10% agarose pads and immobilized in 20 mM levamisole (Sigma-Aldrich). Pictures were captured using a 60x objective (NA 1.45) with an Olympus FV-3000 confocal microscope (Olympus Corporation, Tokyo, Japan) at 5x digital zoom. Three frames of GFP and RFP signals were captured before photobleaching. The values of the fluorescence punctum were calculated by ImageJ software (National Institutes of Health, Bethesda, MD, USA). UNC-49B-A2loop FRAP curves were calculated in Prism 6.0 (GraphPad, San Diego, CA, USA) with a single exponential function.

### Statistical Analyses

All data are presented as the mean ± SEM and passed the D'Agostino-Pearson omnibus and Shapiro-Wilk normality test. Statistical tests of significance were calculated by 1-way ANOVA followed by a post hoc Bonferroni test. Statistical analyses were performed using Prism 6.0 (GraphPad) software. $P < 0.05$ represents the criterion for statistical significance.

## Results

### Identification of *FRMD7* Mutations in Three Chinese Families with INS

Three Chinese families with INS (Figs. 1A–C) were identified and diagnosed by ophthalmologic examinations, and clinical data are shown in Supplementary notes, including Supplementary Table S1, and Supplementary Figure S1.

As *FRMD7* mutations are the primary cause of INS, Sanger sequencing was performed directly to screen all exons and exon-intron boundaries of *FRMD7* in the three families. Ultimately, we identified a duplication mutation (Fig. 1D) in family 1 and two missense mutations in families 2 and 3 (Figs. 1E, 1F), respectively.

In family 1, the novel duplication mutation c.998dupA was identified in the proband (Figs. 1A, III:14, 1D) that results in premature termination at codon 334, and produces a truncated protein (p.His333Glnfs*2). The c.998dupA mutation was also detected in other patients (Fig. 1A, II:4, II:7, III:2, III:5, III:11, III:30, IV:4, IV:13, and IV:20). No mutation was found in healthy individuals (Fig. 1A, III:10, III:13, III:15, III:16, III:17, III:18, III:29, and IV:14). In family 2, the novel missense mutation c.580G>A that results in a substitution of an alanine residue by a threonine at codon 194 (p.Ala194Thr) was found in the proband (Figs. 1B, IV2, 1E). The mutation c.580G>A was also found in other patients (Fig. 1B, II:2 and III:4) but not in healthy individuals (Figs. 1B, III:1, 1E). In family 3, another missense mutation c.973A>G that results in a substitution of an arginine residue by a glycine at codon 325 (p.Arg325Gly) was found in the proband (Figs. 1C, IV:7, 1F). The mutation c.973A>G was also detected in other patients (Fig. 1C, III:1, III:3, III:5, IV:9, IV:13, and V:4) and an asymptomatic female carrier (Fig. 1C, IV:5). No mutation was found in the other four healthy individuals (Fig. 1C, IV:1, V:3, V:5, and V:7). Two female patients (Fig. 1C, IV:9 and IV:13) carry the heterozygous mutation, whereas two healthy female patients (Fig. 1C, IV:5 and IV:12) also carry the heterozygous mutation, which indicate an incomplete penetrance of this mutation in family 3. All three mutations were not found in 50 Chinese female and 100 Chinese male controls.

The p.His333Glnfs*2 mutation may lead to a truncated protein with an incomplete FERM-adjacent (FA) domain and deletion of the full C-terminal domain. The p.Ala194Thr and p.Arg325Gly mutations are located in the highly conserved FERM and FA domains. Sequence blast revealed the Ala194 and Arg325 residues of FRMD7 are highly conserved from humans (*Homo sapiens*) to nematodes (*C. elegans*) (Fig. 1G). The p.Ala194Thr and p.Arg325Gly mutations are predicted to be deleterious by Polyphen-2 (p.Ala194Thr, score = 0.998; p.Arg325Gly, score = 0.575) and SIFT (p.Ala194Thr, score = 0; p.Arg325Gly, score = 0).

Further explorations are required to uncover how these mutations disrupt the physiological function of FRMD7.

### Expression and Localization Analysis of FRMD7 Mutants

To explore whether the three mutations alter the expression of FRMD7, we transfected FRMD7 expressing plasmids into cultured cells. In COS7 cells, we found that the expression

Investigative Ophthalmology & Visual Science

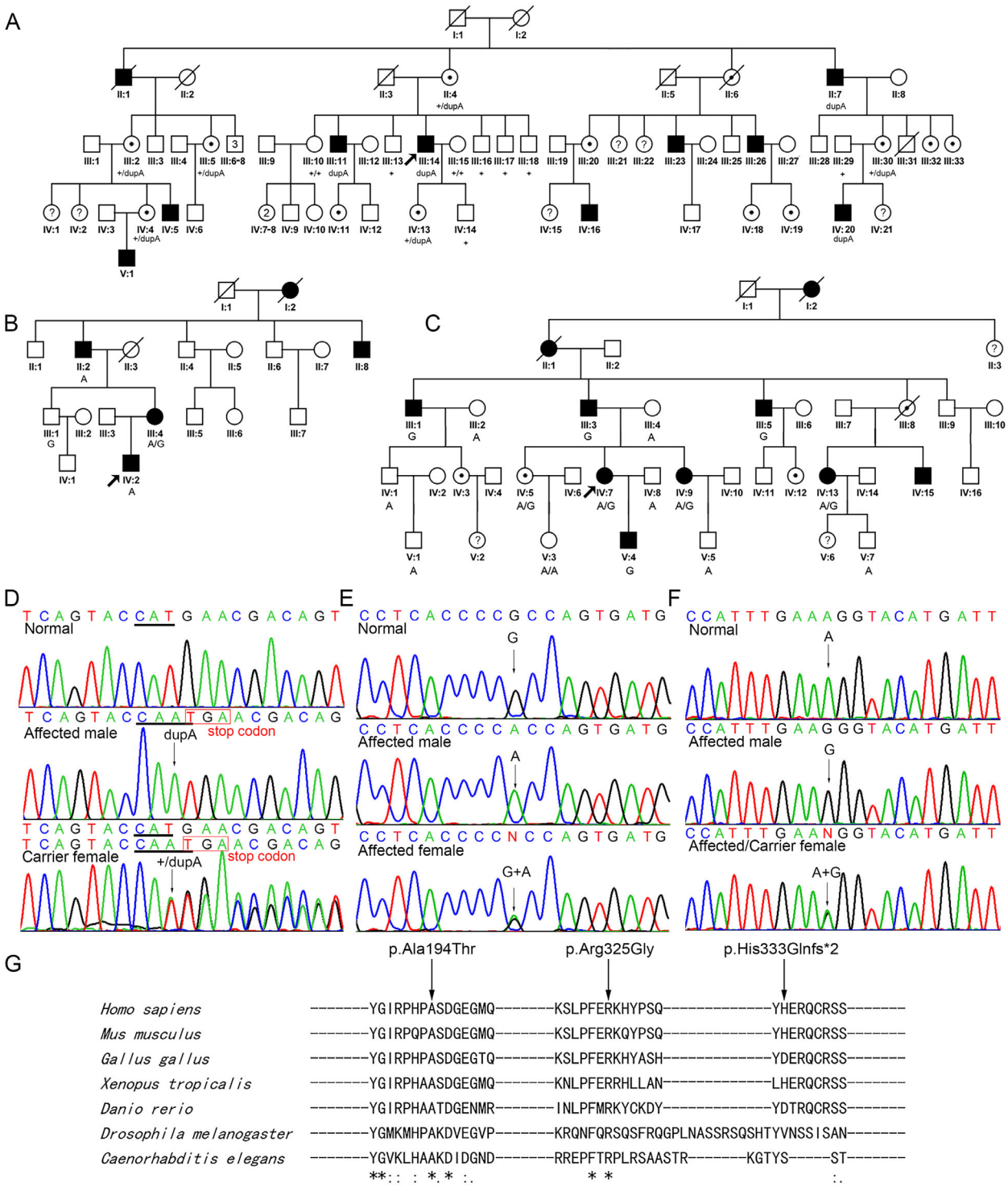


**Figure 1.** Pedigree analysis and molecular genetic analysis of three Chinese families with INS. (**A**) Pedigree structure of family 1. A *square* represents a male individual, a *circle* represents a female individual, an *unfilled symbol* represents a normal phenotype, a *filled symbol* represents an affected phenotype, a *symbol containing a dot* represents a carrier, a *symbol containing a question mark* represents an uncertain genotype, a *symbol with a slash* represents a deceased individual. The proband is marked with an *arrow*. (**B**) Pedigree structure of family 2. (**C**) Pedigree structure of family 3. (**D**) A novel mutation, c.998dupA, of the *FRMD7* gene was identified in family 1. The *arrow* indicates the nucleotide where the mutation occurs. (**E**) The novel mutation c.580G>A in the *FRMD7* gene was identified in family 2. The *arrow* indicates the position where the mutation occurs. (**F**) A mutation c.973A>G of the *FRMD7* gene was identified in family 3. The *arrow* indicates the nucleotide where the mutation occurs. (**G**) The mutated residues p.Ala194 and p.Arg325 are evolutionarily conserved from humans (*Homo sapiens*) to nematodes (*C. elegans*).

Investigative Ophthalmology & Visual Science

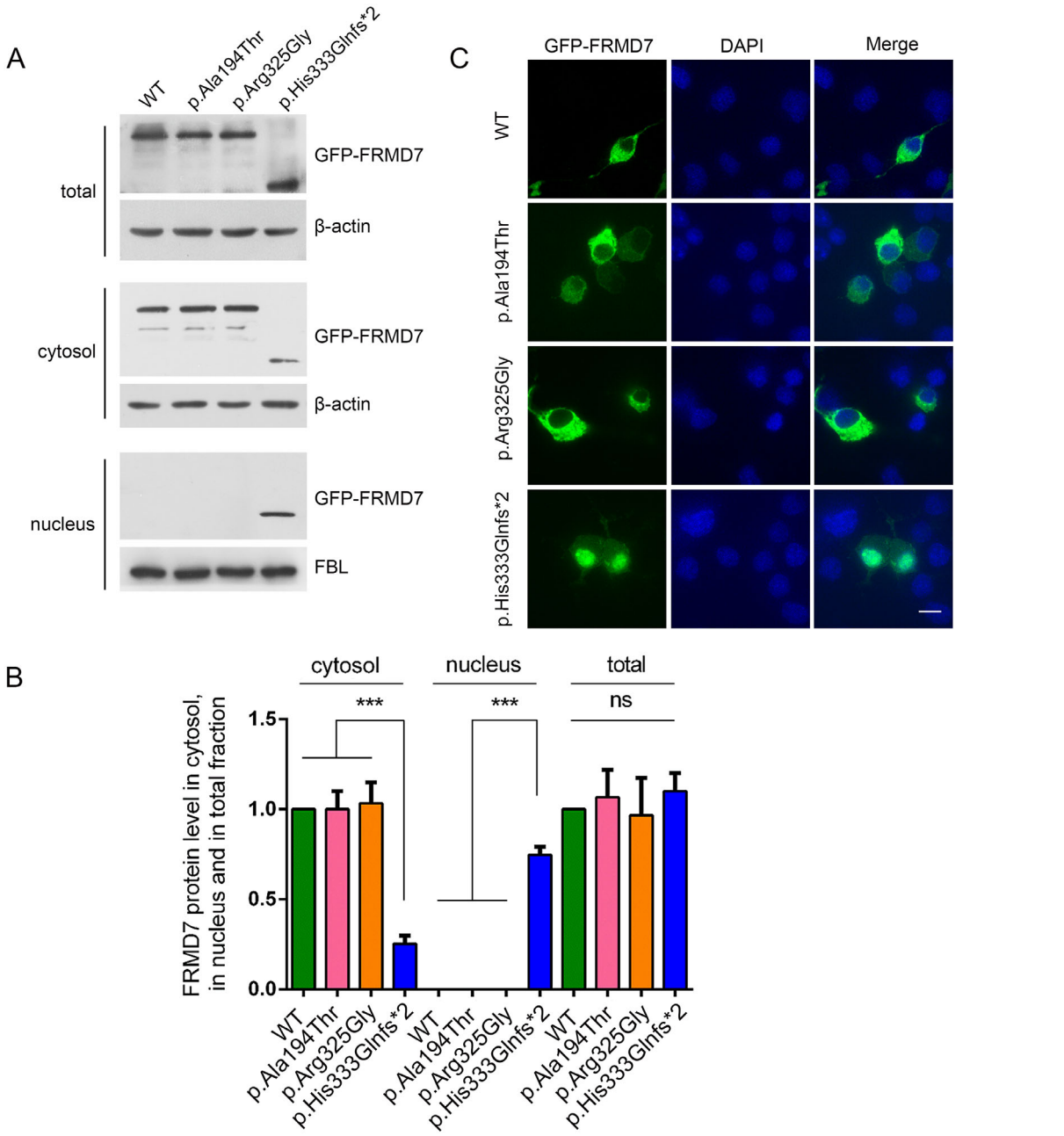


**Figure 2.** Expression and localization of wild-type and three mutant FRMD7. (**A**) Exogenous (total, cytosol, nucleus) protein expression of GFP-tagged wild-type FRMD7 and three mutants in COS7 cells was assessed by Western blotting. Original films are shown in Supplementary Figure S5. (**B**) Quantification of the ratio of GFP-FRMD7/$\beta$-actin and GFP-FRMD7/FBL was detected by Western blotting and normalized to the value obtained from GFP-FRMD7. The data are presented as the mean ± SEM (***$P < 0.001$, ns = nonsignificant) using 1-way ANOVA with Bonferroni post hoc comparisons. (**C**) Localization of wild-type and mutant FRMD7 in N2A cells. Representative images demonstrate that the GFP-tagged wild-type FRMD7 (*green*), as well as the mutants p.Ala194Thr and p.Arg325Gly, are primarily located in the cytoplasm; the p.His333Glnfs*2 mutant is mainly located in the cell nucleus (*Scale bar*, 20 µm). FBL, fibrillarin; WT, wild-type.

levels of the three mutants were similar to the wild-type FRMD7 protein by Western blot analysis (Figs. 2A, 2B). The p.His333Glnfs*2 mutant was substantially present in the nuclear extracts and weakly detected in cytoplasmic extracts, whereas the wild-type FRMD7 and two missense mutants (p.Ala194Thr and p.Arg325Gly) were detected only in the cytoplasmic extracts (Figs. 2A, 2B). Moreover, we expressed GFP-tagged FRMD7 proteins in N2A cells and found that the p.His333Glnfs*2 mutant was predominantly located in the nucleus, whereas the wild-type FRMD7, as well as the mutants p.Ala194Thr and p.Arg325Gly, were primarily located in the cytoplasm (Fig. 2C). These results showed that the p.His333Glnfs*2 mutant was restricted in the nucleus, which may be because the truncated protein cannot be transported to the cytoplasm.[8] Therefore the p.His333Glnfs*2 mutant could lead to loss of FRMD7 function in the cytoplasm. However, how the p.Ala194Thr and p.Arg325Gly mutations impair the function of FRMD7 remains unclear.

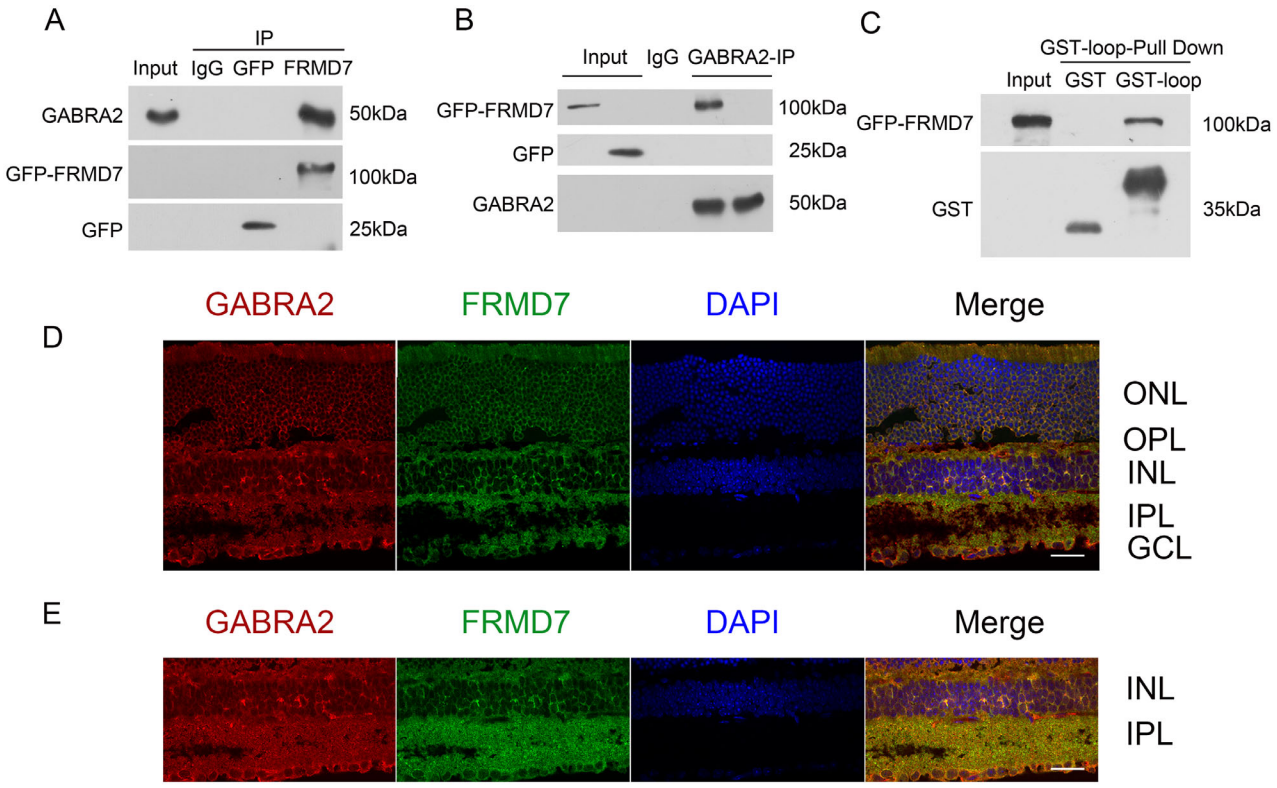


**Figure 3.** FRMD7 binds to the loop between TM3 and TM4 of GABRA2. (**A**, **B**) Interaction between GFP-FRMD7 (expressed in COS7 cells) and full-length GABRA2 (extracted from mouse retina) was verified through IP assays. Original films are shown in Supplementary Figures S6 and S7. (**C**) Direct interaction between FRMD7 and the TM3-TM4 loop of GABRA2 was detected by GST pull-down assays. Original films are shown in Supplementary Figure S8. (**D**) Colocalization of FRMD7 and GABRA2 in the IPL and INL of the mouse retina is demonstrated by immunofluorescent staining and confocal imaging. ONL is the outer nuclear layer, OPL is the outer plexiform layer, INL is the inner nuclear layer, IPL is the inner plexiform layer, and GCL is the ganglion cell layer (*Scale bar*, 20 µm). (**E**) Confocal images showing INL and IPL (*Scale bar*, 20 µm).

## Identification of a Novel Interaction Between FRMD7 and GABRA2

Recently, inhibitory GABAergic signals from SACs to DSGCs were found to be lost in *Frmd7*$^{tm}$ mice,[10] whereas *Gabra2* knockout mice exhibited a similar phenotype (i.e., loss of DS response) as *Frmd7*$^{tm}$ mice,[21] which raises the possibility that FRMD7 and GABRA2 may function in the same pathway to maintain GABAergic signaling in the retina. To explore the association between FRMD7 and GABRA2, we tested whether FRMD7 interacts with GABRA2 using IP assays. We found that exogenous FRMD7 (expressed in cultured cells) coimmunoprecipitated with endogenous GABRA2 (mouse retina protein extracts) and vice versa (Figs. 3A, 3B). FRMD7 is located in the cytoplasm, and GABRA2 has only one functional cytoplasmic loop between TM3 and TM4. Therefore a GST pull-down assay was performed to detect interaction between FRMD7 and the loop of GABRA2. As expected, we found that FRMD7 binds directly to the cytoplasmic loop of GABRA2 (Fig. 3C). To further confirm this interaction, we performed an immunofluorescent experiment and found colocalization of FRMD7 and GABRA2 in the inner plexiform layer (IPL), as well as the inner nuclear layer (INL) of the mouse retina (Figs. 3D, 3E). We analyzed retina images and calculated the average fluorescent level of FRMD7 in different layers (Supplementary Fig. S2) and found that the average level of FRMD7 in INL, IPL, and ganglion cell layers is higher than other layers.

## FRMD7 Mutations Disrupted the Interaction with GABRA2

To investigate how the mutations impaired the interaction between FRMD7 and GABRA2, COS7 cells were cotransfected with FRMD7 and GABRA2 plasmids. We found colocalization of wild-type FRMD7 and GABRA2 in COS7 cells, whereas the truncated mutant p.His333Glnfs*2 did not colocalize with GABRA2 (Fig. 4A). Moreover, the p.Ala194Thr and p.Arg325Gly mutants significantly decreased the interaction with the TM3-TM4 loop of GABRA2 compared with wild-type FRMD7 on GST-pull-down assays (Figs. 4B, 4C).

The results obtained from in vitro assays provide a potential clue to uncover the pathological mechanism of the FRMD7 mutants (i.e., disrupted interaction between FRMD7 and GABRA2), which requires further investigations in vivo.

## FRMD7 Mutants Exhibit a Decreased Rescue Effect in Vivo

FRM-3 is a homologue of human FRMD7 (hFRMD7) in *C. elegans* and was reported to interact with the TM3-TM4 loop of the nematode $GABA_A$ receptor subunit UNC-49B.[27] The protein sequence identity between the FERM domains of FRMD7 and FRM-3 is 46.98% (Supplementary Fig. S3). To verify whether hFRMD7 has function similar to that of FRM-3, *hFRMD7* was expressed in *frm-3* null *C. elegans* by injecting plasmids encoding hFRMD7-GFP or

Investigative Ophthalmology & Visual Science

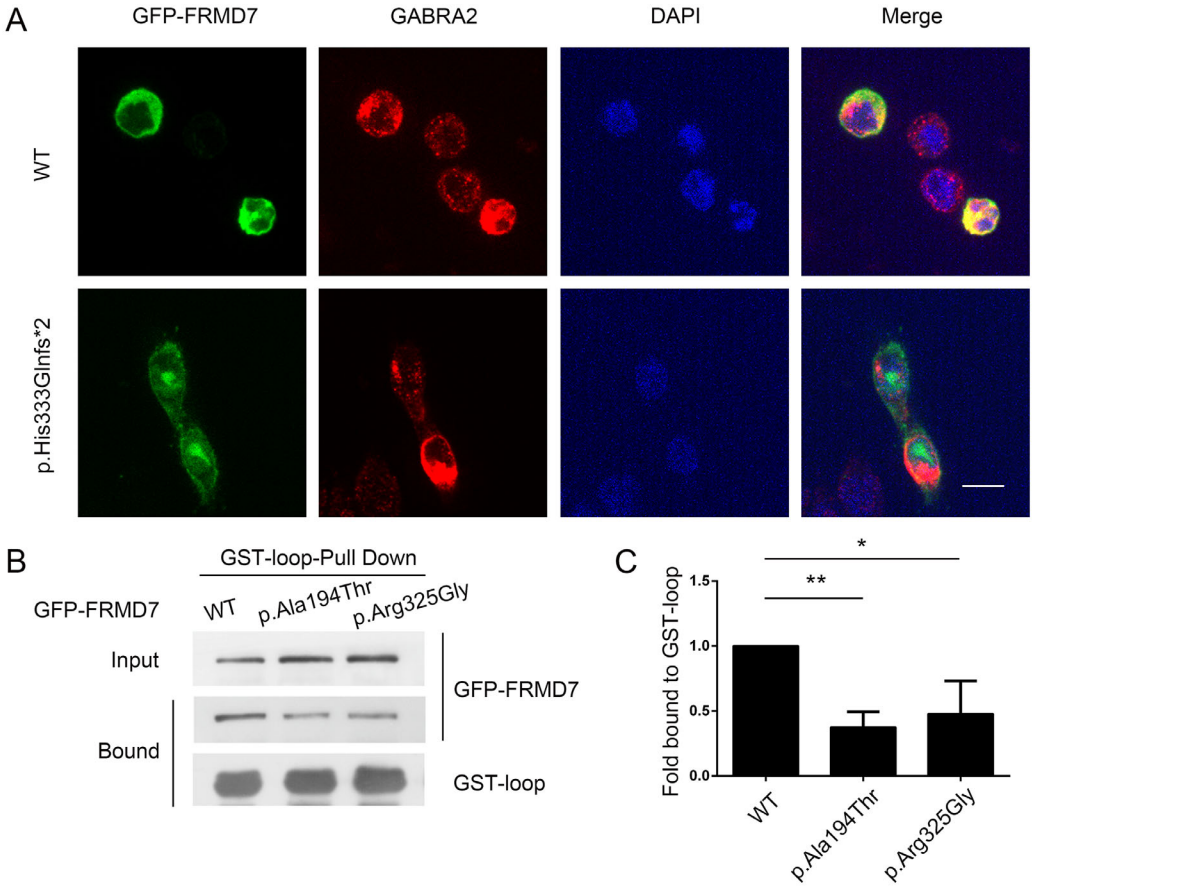


**Figure 4.** FRMD7 mutations disrupt interaction with GABRA2. (**A**) Colocalization of GABRA2 and wild-type FRMD7, but not the mutant p.His333Glnfs*2, is observed in COS7 cells (*Scale bar*, 20 µm). (**B**) The mutations p.Ala194Thr and p.Arg325Gly decrease the binding affinity of FRMD7 to the TM3-TM4 loop of GABRA2. Original films are shown in Supplementary Figure S9. (**C**) Quantification of the binding affinity of FRMD7 bound to GST-GABRA2-LOOP, which is normalized to the value obtained from GFP-FRMD7. The data are presented as the mean ± SEM (*$P < 0.05$, **$P < 0.01$) using 1-way ANOVA with Bonferroni post hoc comparisons. WT, wild-type.

FRM-3-GFP into *frm-3* null *(gk585)* worms. The *frm-3* null worms exhibited decreased locomotion compared with wild-type worms (Fig. 5A; Supplementary Video S1), and expression of FRM-3-GFP fully rescued these locomotion defects, whereas expression of wild-type hFRMD7-GFP alone did not rescue the locomotion defects (Fig. 5A; Supplementary Videos S1–S9, related to nine pictures in Fig. 5A). To address this failure to rescue by hFRMD7, we tested for interaction between hFRMD7 and UNC-49B by GST pull-down assays, and no interaction was detected (data not shown). For further investigation, we generated an artificial UNC-49B protein named UNC-49B-A2loop, which contains an extra human GABRA2 TM3-TM4 loop (Fig. 5B). Expression of the UNC-49B-A2loop protein alone in *frm-3* null worms exhibited no rescue effect on locomotion defect. Interestingly, coexpression of the UNC-49B-A2loop protein together with wild-type hFRMD7 could partially rescue the defect of the locomotion of the *frm-3* null worms (Figs. 5A, 5C, 5D). However, the hFRMD7 mutants p.Ala194Thr, p.Arg325Gly, and p.His333Glnfs*2 exhibited weaker rescue effects than wild-type hFRMD7 (Figs. 5C, 5D). In addition, we assessed the expression patterns of wild-type and mutant hFRMD7 protein in *C. elegans* by Western blotting and found no significant difference between the wild-type and mutants, suggesting that these differences in rescue effects were not due to different expression patterns (Supplementary Fig. S4).

The body muscle cells of *C. elegans* receive both inhibitory GABAergic and excitatory cholinergic signals from motor neurons to maintain the sinusoid pattern, which ensures efficient feeding and optimal survival.[28] To further explore the precise role of hFRMD7 in GABAergic signaling, we performed a FRAP experiment in the dorsal nerve cord of *C. elegans*. When hFRMD7-GFP was expressed under the *frm-3* promoter and UNC-49B-A2loop-RFP was expressed under the *unc-49* promoter, UNC-49B-A2loop-RFP puncta colocalized with hFRMD7-GFP at GABAergic synapses (Figs. 6A, 6B). UNC-49B-A2loop-RFP exhibited similar FRAP characteristics (Figs. 6C, 6D) as UNC-49B, as reported previously.[27] In wild-type worms, 53.8% ± 1.8% of UNC-49B-A2loop-RFP puncta fluorescence was mobile, whereas 78.4% ± 2.4% was mobile in *frm-3* null worms (Figs. 6C, 6D). Expression of wild-type hFRMD7 in *frm-3* null worms stabilized the receptors with 61.2% ± 2.4% mobile puncta, whereas expression of hFRMD7 p.Ala194Thr and p.Arg325Gly had weaker rescue effects (70.9% ± 1.5% and 69.9% ± 1.8%, respectively) (Figs. 6C, 6D).

## Discussion

In this study, we identified three mutations (a duplicate mutation c.998dupA/p.H333Qfs*2, and two missense mutations c.580G>A/p.Ala194Thr and c.973A>G/p. Arg325Gly)

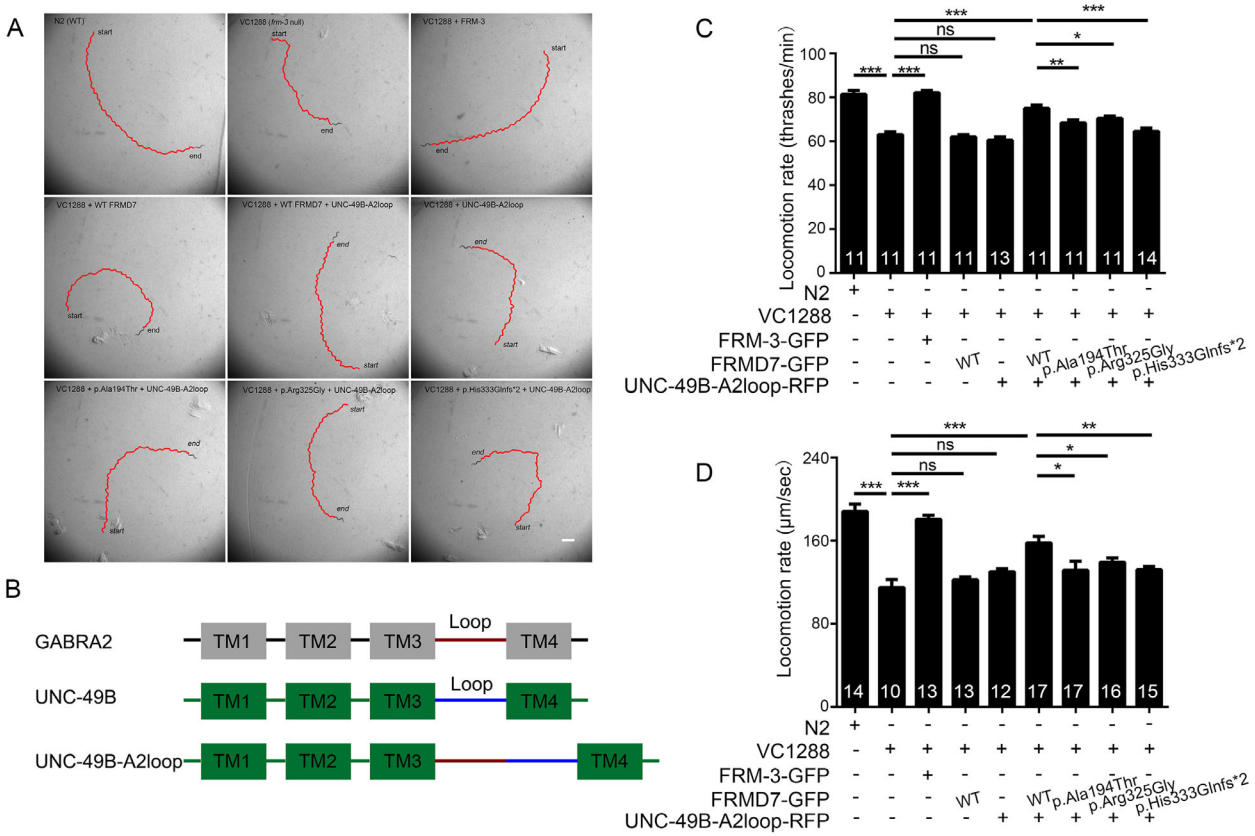


**Figure 5.** FRMD7 mutations impair rescue of the locomotion defect in *frm-3* null *C. elegans*. (**A**) Locomotion tracking of *frm-3* null and transgenic worms on NGM plates for 1 minute. Traces of worm locomotion in 1 minute are outlined in *red*. The start and end represent the start and end positions of individual worms in the recording, respectively (*Scale bar*, 1 mm). (**B**) Schematic structure of GABRA2, UNC-49B, and the artificial protein UNC-49B-A2loop. The TM3-TM4 loop of GABRA2 (*scarlet*) was inserted into the upstream of the TM3-TM4 loop (*blue*) of UNC-49B, forming an artificial cytoplasmic loop. (**C, D**) Quantification of the thrashing and locomotion rates of worms with different genotypes, respectively. Data are the mean ± SEM (**P* < 0.05, ***P* < 0.01, ****P* < 0.001, ns = nonsignificant) using 1-way ANOVA with Bonferroni post hoc comparisons. WT, wild-type.

in *FRMD7* in three Chinese families with INS. Our results identified GABRA2 as a novel binding partner of FRMD7 and demonstrated that pathogenic mutations of FRMD7 lead to decreased binding affinity or loss of colocalization with GABRA2. Furthermore, the pathogenic mutations exhibit a reduced ability to rescue the defects of locomotion and FARP of $GABA_A$Rs in *frm-3* null *C. elegans*.

The common feature in *FRMD7/Frmd7* defective humans and mice is loss of OKR,[5,10,11] which suggests that FRMD7 plays an important role in the genesis of OKR. However, no nystagmus was found in $Frmd7^{tm}$ mice. In humans, horizontal microsaccades may become larger and uncontrolled when the horizontal OKR is lost, appearing as horizontal nystagmus. Mice have not been shown to have microsaccades, which could explain the absence of nystagmus in $Frmd7^{tm}$ mice.[10] Yonehara et al.[10] proposed that the loss of horizontal OKR in $Frmd7^{tm}$ mice is because of the lack of horizontal direction selectivity in the retina, which is caused by defective asymmetric connectivity between SACs and horizontal DSGSs. The defective asymmetric connectivity is manifested as the loss of asymmetry of GABA inhibitory inputs to horizontal DSGCs.[10] We propose that the loss of GABA inhibitory inputs is likely because of the decreased number of immobile $GABA_A$Rs at the synapse. The following evidence supports this hypothesis. First, it has been reported that *Gabra2* knockout mice lost the DS response in DSGC,[21] and Gabra2 is a subunit of $GABA_A$Rs.[24] Second, we found that FRMD7 interacts directly with the loop between TM3 and TM4 of GABRA2 (Figs. 3A, 3B, 3C), and colocalization of FRMD7 and GABRA2 was found in the IPL and INL of the mouse retina (Fig. 3D). Third, FRM-3 (an hFRMD7 homologue) interacts with the loop between TM3 and TM4 of UNC-49B in *C. elegans,* and synaptic $GABA_A$Rs, as well as miniature inhibitory postsynaptic current amplitude, are decreased in *frm-3* null worms.[27] Here we show that FRMD7 together with the loop of GABRA2 could partially rescue the locomotion defects in *frm-3* null worms (Fig. 5) and increases the proportion of immobile UNC-49B-A2loop in the synapse (Fig. 6). Fourth, the INS-associated FRMD7 mutations perturb the interaction between FRMD7 and GABRA2 (Fig. 4) and weaken the rescue effects in *frm-3* null worms (Figs. 5, 6C, 6D). Taken together, these results suggest that FRMD7 interacts with GABRA2 to stabilize immobile $GABA_A$Rs at synapses where SACs connect to DSGCs and that disruptions of this interaction may result in decreased number of immobile $GABA_A$Rs at synapses and further impair GABA inhibitory inputs to DSGCs, eventually leading to the loss of OKR, which is believed to participate in INS.[5,11,33–35] Thus we speculate that FRMD7 mutations disrupt the interaction with GABRA2, and further lead to the loss of OKR that may result in INS.

In *C. elegans*, the 19 D-type GABAergic motor neurons inhibit contraction of the ventral and dorsal body wall muscles during locomotion. A bend in the body is made by contracting muscles via acetylcholine (ACh) innervation on one side of the body while relaxing muscles via GABA

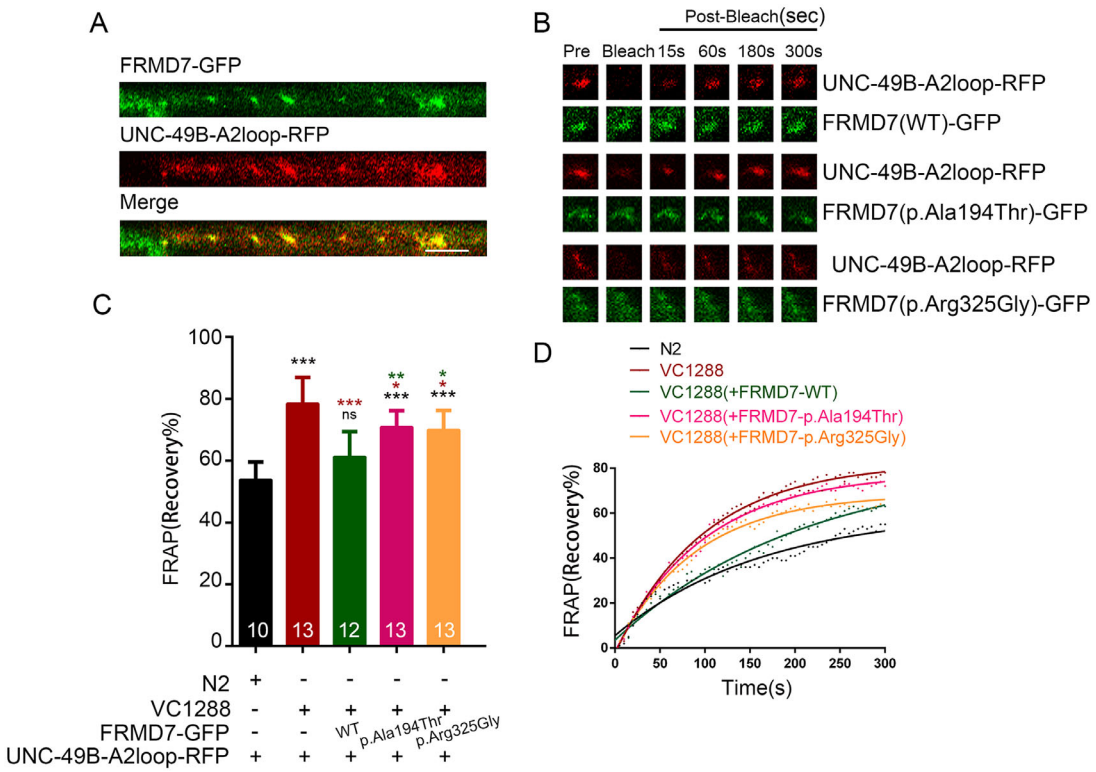


**Figure 6.** FRMD7 mutants show decreased ability to rescue the FRAP defect of $GABA_A$Rs in *frm-3* null *C. elegans*. (**A**) Both FRMD7-GFP (*green*) and UNC-49B-A2loop-RFP (*red*) are expressed in GABAergic neuromuscular junction. Colocalization of fluorescence puncta was chosen for FRAP experiments. (**B**) Representative pictures of UNC-49B-A2loop-RFP FRAP. (**C**) Quantitative data for fluorescence recovery of UNC-49B-A2loop-RFP at 300 seconds after photobleaching. These data are presented as the mean ± SEM (*$P < 0.05$, **$P < 0.01$, ***$P < 0.001$, ns = nonsignificant) using 1-way ANOVA with Bonferroni post hoc comparisons. (**D**) Representative scatter plots of fluorescence recovery. WT, wild-type.

innervation on the opposite side, which gives the worm its distinctive sinusoidal body posture,[28] and we found a decreased locomotion phenotype in *frm-3* null *C. elegans*, which may be because of the uncoordinated ACh and GABA signaling to the body muscles.[27] In humans, a mixed ACh/GABA transmission from the SACs to the DSGCs are believed to play a central role in direction coding in the retina.[19] The loss of OKR in mice and human is likely because of the uncoordinated ACh and GABA signals in retina cells,[10] which may be responsible for the ocular-motor phenotype in FRMD7 patients. Taken together, in both worm and human, the balance of ACh and GABA signaling is critical for physiological function.

Pedigree analysis showed that the inheritance pattern of family 1 (p.H333Qfs*2) is X-linked recessive, whereas both family 2 (p.Ala194Thr) and family 3 (p.Arg325Gly) are X-linked dominant, with incomplete penetrance observed in family 3. The penetrance of FRMD7 mutations in different families is variable,[8,36] but the mechanism of this incomplete penetrance remains unclear. In this study, FRMD7 mutants showed different modes or variable degrees of disruptions in the interaction with GABRA2 (Fig. 4), which may contribute to incomplete penetrance.

## Conclusions

Our work identified a novel interaction between FRMD7 and GABRA2, which might reveal new insight regarding the pathogenesis of INS, and the GABA signal transduced by $GABA_A$Rs might be a novel target for further therapeutic research.

## *Acknowledgments*

The authors thank all the family members for their enthusiastic participation in this study.

Supported by the National Natural Science Foundation of China Grants (31671301, 31871262; JYL), (31701083; YL), and the National Key R&D Program of China (2016YFC1306000; JYL).

Disclosure: **L. Jiang**, None; **Y. Li**, None; **K. Yang**, None; **Y. Wang**, None; **J. Wang**, None; **X. Cui**, None; **J. Mao**, None; **Y. Gao**, None; **P. Yi**, None; **L. Wang**, None; **J. Y. Liu**, None

## *References*

1. Liu JY, Ren X, Yang X, et al. Identification of a novel GPR143 mutation in a large Chinese family with congenital nystagmus as the most prominent and consistent manifestation. *J Hum Genet*. 2007;52:565–570.
2. Rim JH, Lee S, Gee HY, et al. Accuracy of next-generation sequencing for molecular diagnosis in patients with infantile nystagmus syndrome. *JAMA Ophthalmol*. 2017;135:1376.
3. Self J, Lotery A. A review of the molecular genetics of congenital idiopathic nystagmus (CIN). *Ophthalmic Genet*. 2009;28:187–191.
4. Tarpey P, Thomas S, Sarvananthan N, et al. Mutations in FRMD7, a newly identified member of the FERM family,

cause X-linked idiopathic congenital nystagmus. *Nat Genet*. 2006;38:1242–1244.
5. Thomas S, Proudlock FA, Sarvananthan N, et al. Phenotypical characteristics of idiopathic infantile nystagmus with and without mutations in FRMD7. *Brain*. 2008;131:1259–1267.
6. AlMoallem B, Bauwens M, Walraedt S, et al. Novel FRMD7 mutations and genomic rearrangement expand the molecular pathogenesis of X-linked idiopathic infantile nystagmus. *Invest Ophthalmol Vis Sci*. 2015;56:1701–1710.
7. Choi JH, Jung JH, Oh EH, et al. Genotype and phenotype spectrum of FRMD7-associated infantile nystagmus syndrome. *Invest Ophthalmol Vis Sci*. 2018;59:3181–3188.
8. Watkins RJ, Patil R, Goult BT, Thomas MG, Gottlob I, Shackleton S. A novel interaction between FRMD7 and CASK: evidence for a causal role in idiopathic infantile nystagmus. *Hum Mol Genet*. 2013;22:2105–2118.
9. Thomas MG, Crosier M, Lindsay S, et al. Abnormal retinal development associated with FRMD7 mutations. *Hum Mol Genet*. 2014;23:4086–4093.
10. Yonehara K, Fiscella M, Drinnenberg A, et al. Congenital nystagmus gene FRMD7 is necessary for establishing a neuronal circuit asymmetry for direction selectivity. *Neuron*. 2016;89:177–193.
11. Thomas MG, Crosier M, Lindsay S, et al. The clinical and molecular genetic features of idiopathic infantile periodic alternating nystagmus. *Brain*. 2011;134:892–902.
12. Masseck OA, Hoffmann K. Comparative neurobiology of the optokinetic reflex. *Ann N Y Acad Sci*. 2009;1164:430–439.
13. Soodak RE, Simpson JI. The accessory optic system of rabbit. I. Basic visual response properties. *J Neurophysiol*. 1988;60:2037.
14. Brodsky MC, Dell'Osso LF. A unifying neurologic mechanism for infantile nystagmus. *JAMA Ophthalmol*. 2014;132:761–768.
15. Brodsky MC, Tusa RJ. Latent nystagmus: vestibular nystagmus with a twist. *Arch Ophthalmol*. 2004;122:202–209.
16. Distler C, Hoffmann KP. Animal models for the optokinetic system of the human. *Klin Monatsbl Augenh*. 1999;215:78.
17. Straube A, Bronstein A, Straumann D. Nystagmus and oscillopsia. *Eur J Neurol*. 2012;19:6–14.
18. Tarnutzer AA, Straumann D. Nystagmus. *Curr Opin Neurol*. 2018;31:74–80.
19. Sethuramanujam S, McLaughlin AJ, DeRosenroll G, Hoggarth A, Schwab DJ, Awatramani GB. A central role for mixed acetylcholine/GABA transmission in direction coding in the retina. *Neuron*. 2016;90:1243–1256.
20. Hillier D, Fiscella M, Drinnenberg A, et al. Causal evidence for retina-dependent and -independent visual motion computations in mouse cortex. *Nat Neurosci*. 2017;20:960–968.
21. Auferkorte ON, Baden T, Kaushalya SK, et al. GABA(A) receptors containing the alpha2 subunit are critical for direction-selective inhibition in the retina. *PLoS One*. 2012;7:e35109.
22. Bedford FK, Kittler JT, Muller E, et al. GABA(A) receptor cell surface number and subunit stability are regulated by the ubiquitin-like protein Plic-1. *Nat Neurosci*. 2001;4:908–916.
23. Jacob TC. Gephyrin regulates the cell surface dynamics of synaptic GABAA receptors. *J Neurosci*. 2005;25:10469–10478.
24. Jacob TC, Moss SJ, Jurd R. GABAA receptor trafficking and its role in the dynamic modulation of neuronal inhibition. *Nat Rev Neurosci*. 2008;9:331–343.
25. Loebrich S, Bahring R, Katsuno T, Tsukita S, Kneussel M. Activated radixin is essential for GABAA receptor alpha5 subunit anchoring at the actin cytoskeleton. *Embo J*. 2006;25:987–999.
26. Tretter V, Jacob TC, Mukherjee J, Fritschy JM, Pangalos MN, Moss SJ. The clustering of GABAA receptor subtypes at inhibitory synapses is facilitated via the direct binding of receptor 2 subunits to gephyrin. *J Neurosci*. 2008;28:1356–1365.
27. Tong X, Hu Z, Liu Y, Anderson D, Kaplan JM. A network of autism linked genes stabilizes two pools of synaptic GABAA receptors. *Elife*. 2015;4:e09648.
28. Girard LR, Fiedler TJ, Harris TW, et al. WormBook: the online review of *Caenorhabditis elegans* biology. *Nucleic Acids Res*. 2007;35:D472–D475.
29. Maity R, Pauty J, Krietsch J, Buisson R, Genois MM, Masson JY. GST-His purification: a two-step affinity purification protocol yielding full-length purified proteins. *J Vis Exp*. 2013:e50320.
30. Brenner S. The genetics of *Caenorhabditis elegans*. *Genetics*. 1974;77:71–94.
31. Mello CC, Kramer JM, Stinchcomb D, Ambros V. Efficient gene transfer in *C. elegans*: extrachromosomal maintenance and integration of transforming sequences. *EMBO J*. 1991;10:3959–3970.
32. Miller KG, Alfonso A, Nguyen M, Crowell JA, Johnson CD, Rand JB. A genetic selection for *Caenorhabditis elegans* synaptic transmission mutants. *Proc Natl Acad Sci U S A*. 1996;93:12593–12598.
33. Huang Y, Rinner O, Hedinger P, Liu S, Neuhauss SCF. Oculomotor instabilities in zebrafish mutant belladonna: a behavioral model for congenital nystagmus caused by axonal misrouting. *J Neurosci*. 2006;26:9873–9880.
34. Traber GL, Chen C, Huang Y, et al. Albino mice as an animal model for infantile nystagmus syndrome. *Invest Ophth Vis Sci*. 2012;53:5737.
35. Huber-Reggi SP, Chen C, Grimm L, Straumann D, Neuhauss SCF, Huang MY. Severity of infantile nystagmus syndrome-like ocular motor phenotype is linked to the extent of the underlying optic nerve projection defect in zebrafish belladonna mutant. *J Neurosci*. 2012;32:18079–18086.
36. Watkins RJ, Thomas MG, Talbot CJ, Gottlob I, Shackleton S. The role of FRMD7 in idiopathic infantile nystagmus. *J Ophthalmol*. 2012;2012:1–7.

## Supplementary Materials

Videos correspond to Figure 5A.

**Supplementary Video S1.** For N2 (WT) worm.

**Supplementary Video S2.** For VC1288 (*frm-3* null) worm.

**Supplementary Video S3.** For VC1288 expressing FRM-3.

**Supplementary Video S4.** For VC1288 expressing WT FRMD7.

**Supplementary Video S5.** For VC1288 expressing WT FRMD7 and UNC-49-A2loop.

**Supplementary Video S6.** For VC1288 expressing UNC-49-A2loop.

**Supplementary Video S7.** For VC1288 expressing FRMD7 p.Ala194Thr and UNC-49-A2loop.

**Supplementary Video S8.** For VC1288 expressing FRMD7 p.Arg325Gly and UNC-49-A2loop.

**Supplementary Video S9.** For VC1288 expressing FRMD7 p.His333Glnfs*2 and UNC-49-A2loop.

Investigative Ophthalmology & Visual Science